 DOI: 10.1002/masy.200951204

Spectroscopic, Mechanical and Dynamic-Mechanical Studies on the Photo-Aging of a Tetrafunctional Epoxy Resin

Giuseppe Ragosta, Mario Abbate, Pellegrino Musto, Gennaro Scarinzi*

Summary: The photo-oxidative degradation of a densely cross-linked epoxide/diamine network based on tetraglycidyl-4,4′ diaminodiphenylmethane (TGDDM) and 4,4′ diaminodiphenyl sulphone (DDS) has been investigated by FTIR spectroscopy, dynamic-mechanical analysis (DMA) and compressive mechanical tests. The FTIR measurements allowed us to monitor the degradation process of the different groups present in the TGDDM/DDS network and to obtain reliable kinetic data. On this basis the most likely photo-degradation mechanisms were proposed. Dynamic-mechanical measurements and mechanical compressive tests were used to gain an insight in the effect of the photo-oxidative degradation on the relaxation processes of the epoxy network and on the mechanical performances.

Keywords: epoxy resins; FTIR spectroscopy; mechanical properties; relaxation processes

Introduction

Due to their outstanding properties, epoxy resins are a class of materials of primary technological interest. In particular, these resins are characterized by high resistance to chemicals and corrosive agents, good mechanical properties, excellent adhesion to various substrates, low shrinkage upon cure and ease of processing under a wide range of conditions.[1–3] The most important application of epoxy resins is in the transportation industry, particularly in such areas as civil and military aircraft industry, aerospace and in the marine and automotive sectors.[2,4] One of the main concerns when dealing with these applications is the sensitivity to natural weathering, i.e. the effect of prolonged exposure to direct sunlight in an atmospheric environment. It has been demonstrated [4,5] that, under these conditions, bifunctional epoxies based on diglycidyl ether of bisphenol-A (DGEBA) undergo quite extensive photo-degradation which brings about a considerable deterioration of mechanical performances and, ultimately, the failure of the item. Much less information is available on the photo-aging behaviour of resins based on tetraglycidyl-4,4′-diaminodiphenylmethane (TGDDM), although this monomer, cured with the aromatic diamine hardener 4,4′-diaminodiphenyl sulphone (DDS) represents the preferred matrix for carbon fiber composites in aerospace applications.[3] The present contribution is aimed at investigating the kinetics and mechanisms of the photo-degradation process of a TGDDM/DDS network in an experimental set-up simulating the actual service conditions. Moreover, the effect of the photo-degradation on the viscoelastic response of the material and on its mechanical performances is studied in the light of the changes taking place within the molecular structure of the network. The experimental approaches used throughout are Fourier Transform infrared (FTIR) spectroscopy for the kinetic and mechanistic analysis, and dynamic-mechanical

Institute of Chemistry and Technology of Polymers (ICTP), National Research Council of Italy, Via Campi Flegrei 34, 80078 Pozzuoli (Naples), Italy
E-mail: rago@ictp.cnr.it

spectroscopy and compressive mechanical tests for the viscoelastic behaviour and the mechanical properties, respectively.

Experimental Part

The epoxy resin was a commercial grade tetraglycidyl-4,4′-diaminodiphenylmethane (TGDDM) supplied by Ciba Geigy, and the curing agent was 4,4′-diamino-diphenylsulphone (DDS) from Aldrich. The chemical structure of resin components is shown below:

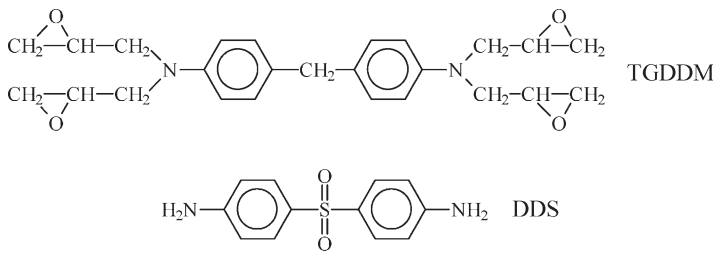

The composition of the reactive mixture was typical of a commercial formulation. Thirty grams of DDS was dissolved in 100 g of TGDDM at 120 °C, degassed under vacuum, and poured between two stainless plates. The first step of the curing schedule was carried out at 140 °C for 16 h, followed by a post-curing step at 200 °C for 4 h. Further details about the sample preparation are reported elsewhere.[6] The photo-aging experiments were carried out at 50 °C and 50% of relative humidity in an environmental chamber equipped with a UV bulb lamp mainly emitting in the spectral range of 320–600 nm (simulating the solar spectrum). Transmission FTIR spectra were obtained using a Perkin-Elmer System 2000 spectrometer. Dynamic-mechanical tests were conduced on samples with dimensions $50 \times 10 \times 1.0$ mm using a Perkin-Elmer Pyris DMA apparatus. The tests were performed from -150 °C to $+350$ °C at a heating rate of 3 °C/min and at 1 Hz. Compressive mechanical tests were carried out on specimens $12 \times 6.0 \times 4.0$ mm at ambient temperature and at a cross-head speed of 1mm/min using an Instron machine model 4505.

Results and Discussion

FTIR Spectroscopy

In Figure 1, trace A is reported the FTIR spectrum of the fully cured TGDDM/DDS resin in the 4000–350 cm^{-1} wavenumber range. The spectrum has been thoroughly discussed in several literature studies [7,8] and, in particular, in ref. 7 assignments have been proposed for most peaks.

The substantial changes occurring in the FTIR spectrum with exposure time are demonstrated in Figure 1, traces B and C. It is apparent that the concentration of aliphatic groups decreases steadily (reduction of the absorbance area of the bands at

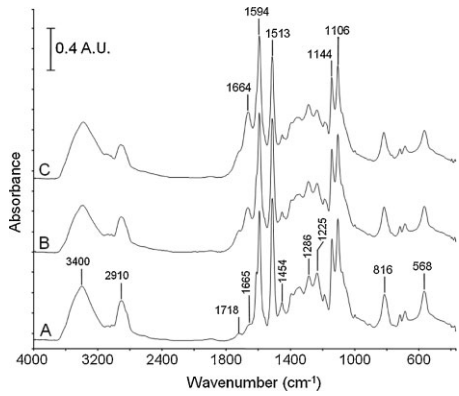

Figure 1.
Transmission FTIR spectra in the wavenumber range 4000–350 cm^{-1} of the TGDDM/DDS resin before and after photo-degradation. Trace A: initial spectrum. Trace B: spectrum after 1.5×10^4 min. Trace C: spectrum after 3.1×10^4 min.

2910 and 1454 cm^{-1}). The concentration of the substituted benzene rings also declines: reduction of the peaks at 1513 cm^{-1} (TGDDM aromatics) and at 1594 cm^{-1} (DDS aromatics). On the other hand, the two carbonyl bands centred at 1718 and 1665 cm^{-1} increase substantially with exposure time. Among the various carbonyl species formed by photo-oxidation the two dimensional FTIR spectroscopy[6] identified essentially amide groups at 1675 cm^{-1}, aldehyde/ketone functionalities at 1728 cm^{-1} and carboxylic acids at 1765 cm^{-1}.

The above spectral data allow a quantitative description of the photo-oxidation process in terms of relative conversion and reaction rates for the reactive groups that are consumed, or as rate of formation for the functionalities (carbonyls) produced upon the oxygen attack on the polymer network. The relative conversion at time t, α_t, can be expressed spectroscopically as:

$$\alpha_t = \frac{C_0 - C_t}{C_0} = 1 - \frac{C_t}{C_0} = 1 - \frac{A_t}{A_0} \qquad (1)$$

The reaction rates can be estimated once an appropriate kinetic model has been identified, as in the forthcoming discussion.

The relative conversion α *vs* time for the peaks at 1454 cm^{-1} (CH_2 groups), 1593 cm^{-1} (DDS aromatics) and 1513 cm^{-1} (TGDDM aromatics) are reported, respectively, in Figure 2 and in Figure 3, curves A and B. In Figure 4 are shown the absorbance *vs* time profiles for the carbonyl components at 1725 and 1665 cm^{-1}.

A phenomenological model widely adopted to describe heterogeneous processes governed by phase-boundary reaction mechanisms has the form[9,10]:

$$\frac{d\alpha}{dt} = Ae^{-\frac{E_a}{RT}}(1-\alpha)^n \qquad (2)$$

Equation 2 is meaningful only for discrete values of n.[9] For $n = 1$, integration of Equation 2 yields:

$$\alpha_t = \alpha_f(1 - e^{-kt}) \qquad (3)$$

where α_f is the final conversion and $k = Ae^{-\frac{E_a}{RT}}$ is the Arrhenius-type, kinetic constant. Furthermore, recalling that

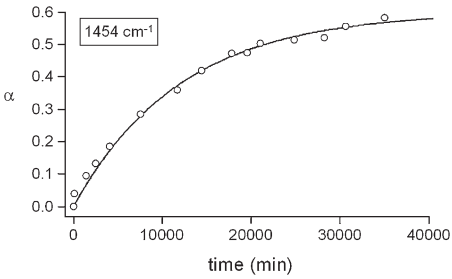

Figure 2.
Relative conversion of the CH_2 groups as a function of photo-degradation time. The empty circles represent experimental data, the continuous line is the kinetic profile obtained by the model Equation 3.

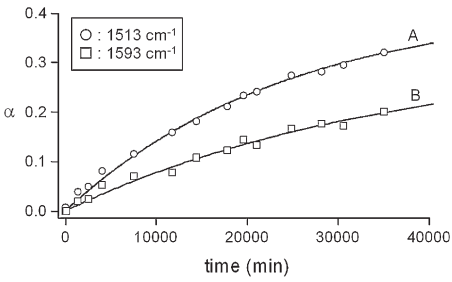

Figure 3.
Relative conversion of the aromatic rings of the TGDDM unit (A) and of the DDS unit (B) as a function of photo-degradation time. The symbols represent experimental data, the continuous lines are the kinetic profiles obtained by the model Equation 3.

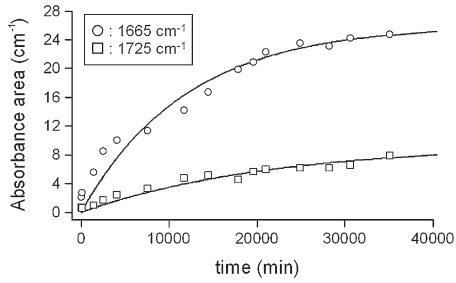

Figure 4.
Absorbance area of the carbonyl peaks as a function of photo-degradation time. The symbols represent experimental data, the continuous lines are the kinetic profiles from model Equation 4.

Table 1.
Kinetic constants (k) and final conversions (or A_f) for the various functional groups involved in the photodegradation process.

Functional group	k ($min^{-1} \times 10^5$)	α_f (%)
CH_2	8.7 ± 0.6	59 ± 1
Ar (TGDDM)	4.1 ± 0.1	42 ± 7
Ar (DDS)	2.7 ± 0.01	32 ± 5
C=O (Amide)	8.9 ± 1	$25^{a)} \pm 1$
C=O (Ketone)	4.6 ± 0.3	$9.5^{a)} \pm 0.5$

[a)] A_f

$\alpha_t = \frac{A_0 - A_t}{A_0}$, the conversion equation can be written as:

$$A_t = A_f(1 - e^{-kt}) \quad (4)$$

when A_0 is zero.[6]

It was found that for all profiles the best fit was achieved with a first order model ($n = 1$), which yielded a very satisfactory description of the experimental data. The curves obtained by Equations 3 or 4 through a non-linear least-square regression of the experimental data are reported, as continuous lines, in Figures 2–4. The kinetic parameters (i.e. rate constants and final conversion) evaluated by the model are collectively reported in Table 1. It is apparent that the kinetic constant (k) relative to the consumption of CH_2 groups has a value close to that relative to the formation of amide groups, while the aldehyde/ketone carbonyls and the two aromatic rings display significantly lower k values. In particular, the carbonyl groups and the TGDDM aromatics display close k values, while the kinetic constant for the DDS aromatics is about 1.7 times lower. Thus, from the kinetic analysis, it emerges

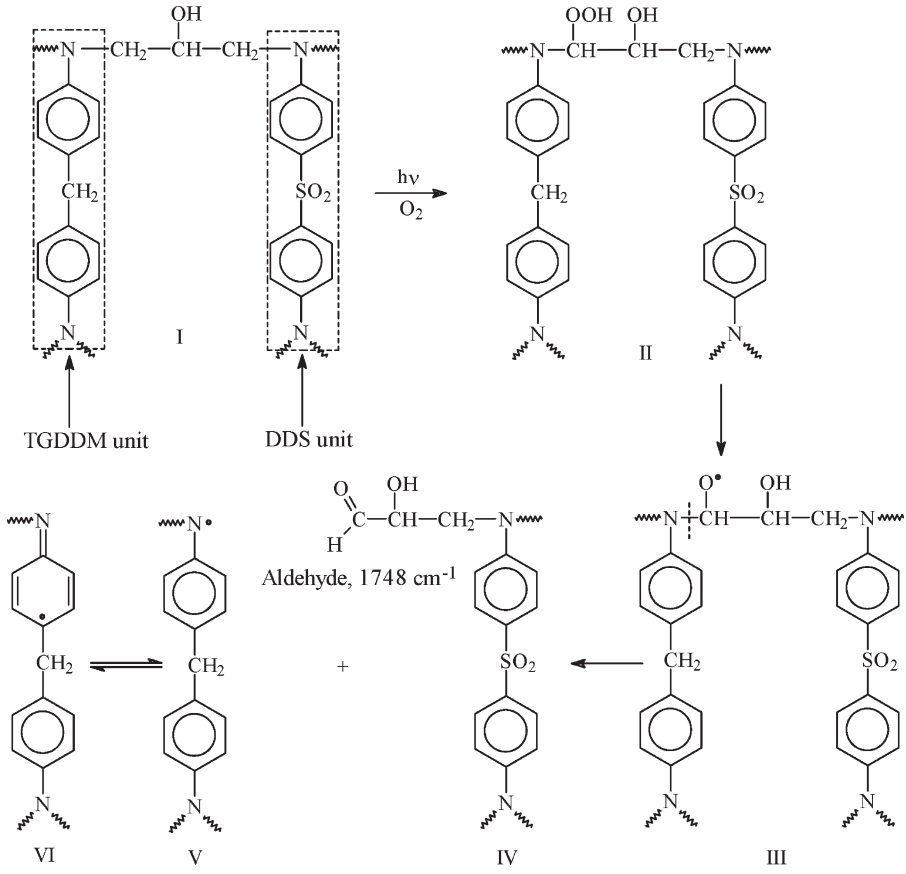

Scheme 1.

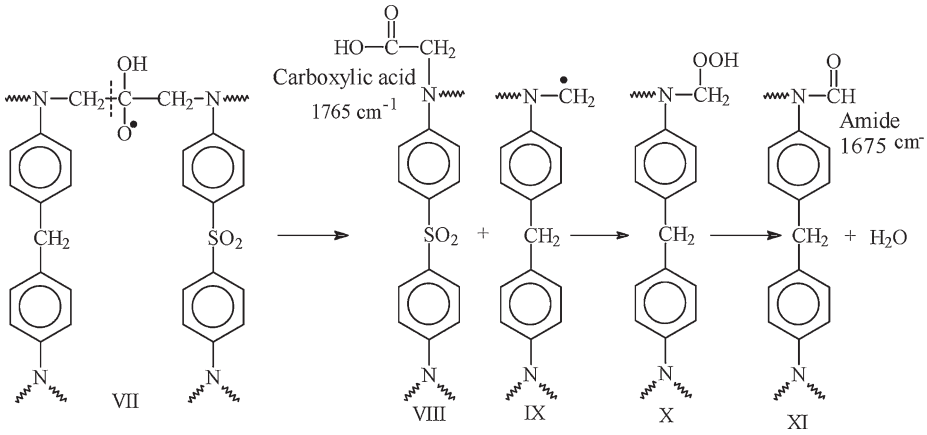

Scheme 2.

that the methylene groups are the more susceptible to photo-oxidation and, possibly, the site of initiation of the whole process.

Proposed Photo-Oxidation Mechanisms

A mechanism to describe the photo-oxidative degradation of the TGDDM/DDS system has to account for the main findings of the spectroscopic analysis. One possible reaction pathway starts by hydrogen abstraction on the methylene group linked to the nitrogen atom, as depicted in Scheme 1.

The resulting hydroperoxide group (structure II) evolves as usual, by thermal decomposition and formation of a peroxy-radical (III). Breaking at the N–C bond produces the aldehyde species detected spectroscopically (structure IV) and the structure V, which is stabilized by resonance. This mechanism also account for the decrease of the aromatic groups' concentration observed spectroscopically. A concurrent degradation mechanism is shown in Scheme 2. The structure VII, formed from structure I through hydrogen abstraction and oxygen attack, may evolve by chain scission at the carbon-carbon bond forming a carboxylic acid (structure VIII, IR signal at 1765 cm^{-1}) and the structure IX which ultimately would produce an amide linkage (structure XI, IR signal at 1675 cm^{-1}). This mechanism, however, cannot be responsi-

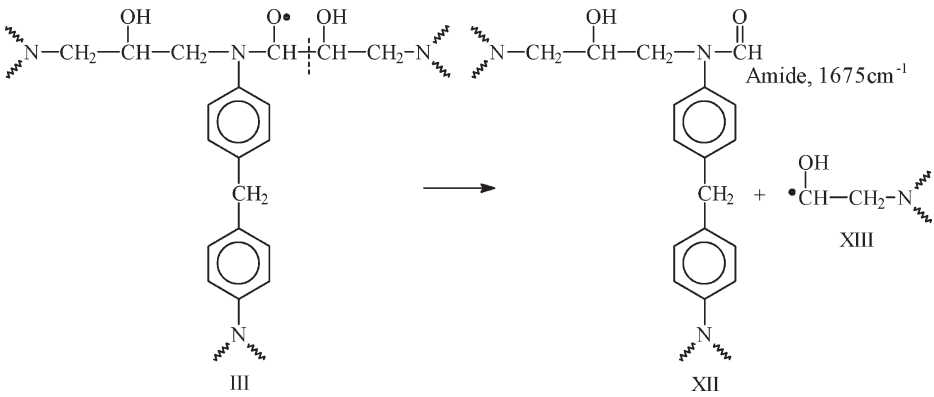

Scheme 3.

ble for the whole production of amide groups in the system, since the spectroscopic data demonstrate that the carboxylic acid concentration is very limited with respect to the other carbonyl species, whereas the amide group concentration is strongly predominant. In a previous paper[6] it was found that the principal route for amide formation starts from the peroxy radical III of Scheme 1, with a chain-scission occurring at the carbon-carbon bond, rather than at the carbon-nitrogen bond (see Scheme 3). In summary, the photo-oxidative degradation of the TGDDM/DDS network is a complex process involving several mechanisms which ultimately bring about chain-scission mainly localized on the aliphatic segment of the network. The mechanisms which are more likely to occur are those leading to amide and carbonyl groups with the amide route largely prevailing, as evidenced by the kinetic analysis.

Dynamic Mechanical Analysis

Dynamic-mechanical spectra in terms of storage modulus (E') and tan δ at 1 Hz for the plain TGDDM/DDS resin and for the same resin photo-oxidized for 600 and 1000 hours are shown in Figures 5a-c. The tan δ plots reveal the occurrence of three distinct relaxation processes at increasing temperatures. In particular, the relaxation at the lowest temperature (Figure 5b) is commonly referred to as the β transition, while the relaxation appearing in the highest temperature region (Figure 5c) is an α-transition process and corresponds to the glass transition temperature (T_g.) In fact, in this region the storage modulus (Figure 5a) shows a sharp drop and then approaches to a rubbery region. The relaxation process between the α and β peaks is denoted ω; its molecular origin is still uncertain.[11,12]

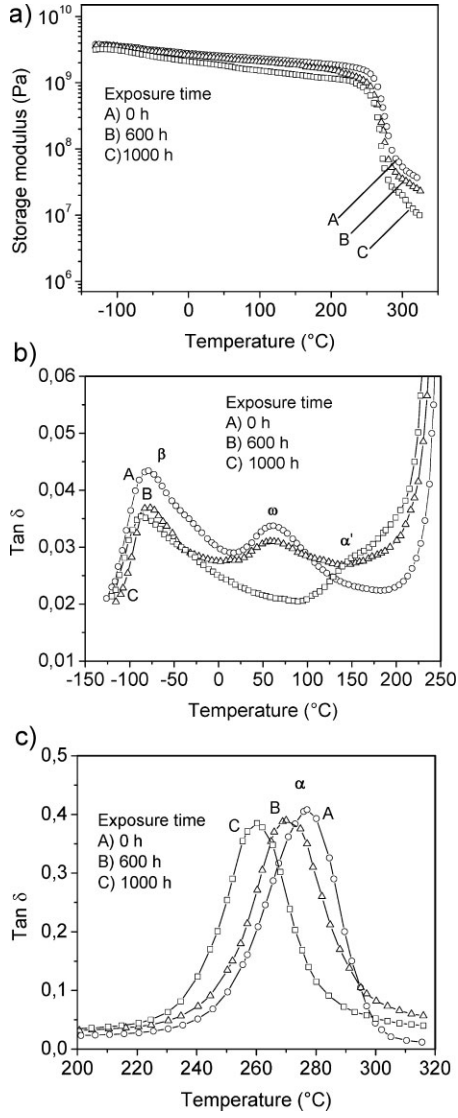

Figure 5.
(a) Storage modulus (E') as a function of temperature. (b) Loss factor (tan δ) as function of temperature in the range −150 °C to 250 °C. (c) Loss factor (tan δ) as function of temperature in the range 200 °C to 320 °C. Exposure time as indicated.

The data of Figure 5 show clearly the changes induced by the photo-oxidative process, which can be summarized as follows:

i) The modulus in the rubbery region decreases markedly with increasing the exposure time. ii) The intensity of β and ω transitions also decreases. iii) The α and β relaxation peaks (T_g and T_β) are shifted to lower temperatures as the exposure time increases, while the position of the ω relaxation peak (T_ω)

Table 2.
Transition temperatures (T_β, T_ω, T_g), rubbery modulus (E'_r), and crosslink density (ν) of TGDDM/DDS resins before and after photo-oxidation.

Exposure time (h)	T_β (°C)	T_ω (°C)	T_g (°C)	E'_r (Pa)	ν (mol cm^{-3})
0	−72.2	62.4	278.0	4.0×10^7	2.7×10^{-3}
600	−78.1	61.5	270.0	3.1×10^7	2.1×10^{-3}
1000	−82.2	–	260.0	2.0×10^7	1.4×10^{-3}

remains essentially unchanged after 600 h. Subsequently at 1000 h this transition becomes barely detectable and a new relaxation, indicates as α', appears in the range 140 °C–200 °C as a shoulder of the principal peak.

In Table 2 are reported the values of T_β, T_ω, and T_g determined from the maxima of the tan δ curves. It can be seen that for the two photo-oxidized samples the decrease in T_g is, respectively, 8 °C and 18 °C, whereas the T_β reduction is of about 6 °C and 10 °C.

It is known that for epoxy resins the peak position and the intensity of the primary and secondary relaxation processes are related to crosslink density.[11,12] Thus, the rubber elasticity theory along with the experimental storage modulus in the rubbery region (E'_r) were used to estimate the cross-link density (ν) of the neat and photo-oxidized epoxy networks.[6,11,13] The values of ν are reported in Table 2. It is found that for the two photo-oxidized samples ν decreases by 22.2% and 48.1% with respect to the original network. This reduction accounts for the marked lowering of the glass transition temperature and, at the same time, indicates that a massive chain scission has occurred during the photo-oxidation process.

In the light of the spectroscopic results, the chain scission processes mainly responsible of the above effect can be identified as those occurring within the aliphatic segment of the network and, in particular, at the carbon–carbon bond (see Scheme 3). Obviously, other mechanisms contribute, as those outlined in Schemes 1 and 2.

With respect to the β transition, the dynamic-mechanical analysis evidences that, in terms of peak shift, the effect of photo-aging is lower than that on the α transition. In order to account for this result, we have to take into consideration the molecular origin of the β transition, which is generally attributed to localized motions of small units of the epoxy network.[14,15] We propose to associate the β relaxation to the rotation of the disubstituted phenyl rings. This interpretation is supported by the value of the activation energy of the transition estimated by a multifrequency analysis.[6] The above assignment also justifies the lower effect of photo-aging, insofar as the degradation mechanisms which produce the disruption of the aromatic rings are to be considered minor reaction pathways.

As far as the ω relaxation is concerned, it has not received great attention in the literature. It has been commonly associated to the local motion of chain segments heavily restricted by crosslinking points.[16,17] Upon degradation (1000 h) the vanishing of the transition can be attributed to the chain-scission which reduces these cross-linking points. The appearance of the α' relaxation is to be related to more cooperative mechanisms involving newly formed dangling chains.

Table 3.
Mechanical properties of TGDDM/DDS resins before and after photo-oxidation.

Exposure time (h)	Modulus (GPa)	Yield strength (MPa)	Strain at yield (%)
0	3.2	179	15.1
600	3.1	160	13.4
1000	3.0	135	11.3

Mechanical Properties

The results related to compressive mechanical tests for the neat and photo-oxidized samples are reported in Table 3. During the test all samples exhibited extensive yielding and were found to deform to strains exceeding 30%. The data of Table 3 show that the elastic modulus is scarcely affected by the photo-oxidation, indicating that this parameter is mainly dependent on the interaction between chains rather than on the crosslink density. On the other hand, the yield strength, evaluated as the stress corresponding to 5% offset from the elastic strain, decreases as the photo-oxidation time increases and is reached at lower deformations. The yield strength, as opposed to modulus, is a high-strain property, and therefore is dependent on the crosslink density. Considering that the yielding is an energy activated process[18] involving movements of molecular segments in the direction of the applied stress, the results of Table 3 indicate that the chain scission reactions lower the energy barrier for yielding to occur, allowing it to take place at lower stress and stain values.

Conclusion

FTIR spectroscopy has allowed us to simultaneously monitor the photo-degradation of several groups present in a TGDDM/DDS network, so as to rank their relative stability. The kinetic analysis demonstrated that all concentration profiles can be suitably described by a phase-boundary model with reaction order equal to one, thus allowing to evaluate the kinetic constants for the main functional groups involved in the process. On the basis of the spectroscopic results the photo-degradation mechanisms which are more likely to occur were proposed and discussed. A dynamic-mechanical analysis was performed to gain an insight in the effect of chain-scission reactions on the viscoelastic properties of the material. Marked reduction of the rubbery modulus, the primary and secondary relaxation temperatures and the crosslink density were found upon photo-degradation. The compressive mechanical test showed a marked reduction of the mechanical performances of the material at high exposure times, especially in terms of yield stress and strain.

[1] H. Lee, K. Neville, *Handbook of Epoxy Resins*, McGraw-Hill, New York 1990.
[2] J. K. Gillham, *Encyclopaedia of Polymer Science and technology*, 2nd ed., John Wiley, New York 1986.
[3] C. A. May, *Epoxy Resins, Chemistry and Technology*, 2nd ed., Marcel Dekker Inc., New York 1988, L.F.
[4] V. Bellenger, J. Verdu, *J. Appl. Polym. Sci.* **1985**, *30*, 363.
[5] V. Bellenger, J. Verdu, *J. Appl. Polym. Sci.* **1983**, *28*, 2599.
[6] P. Musto, G. Ragosta, M. Abbate, G. Scarinzi, *Macromolecole* **2008**, *41*, 5729.
[7] P. Musto, G. Ragosta, P. Russo, L. Mascia, *Macromol. Chem. Phys.* **2001**, *202*, 3445.
[8] R. J. Morgan, E. T. Mones, *J. Appl. Polym. Sci.* **1987**, *33*, 999.
[9] N. Rose, M. Le Bras, S. Bourbigot, R. Delobel, B. Costes, *Polym. Degrad. Stab.* **1996**, *54*, 355.
[10] A. E. Venger, Y. E. Fraiman, F. B. Yurevic, *J. Thermal. Anal.* **1983**, *27*, 325.
[11] T. Sasuga, A. Udagawa, *Polymer*, **1991**, 32, 402.
[12] L. Vignoud, L. David, B. Sixou, G. Vigier, *Polymer*, **2001**, *42*, 4657.
[13] A. C. Grillet, J. Galy, J. F. Gerard, J. P. Pascault, *Polymer*, **1991**, *32*, 1885.
[14] J. D. Keenan, J. C. Seferis, *J. Appl. Polym.* **1979**, *24*, 2375.
[15] O. Becker, R. Varlay, G. Simon, *Polymer*, **2002**, *43*, 4365.
[16] R. G. C. Arridge, J. H. Speak, *Polymer*, **1972**, *25*, 1817.
[17] M. Ochi, M. Shimbo, M. saga, N. Takashima, *J. Polym. Sci.* **1986**, *24*, 2185.
[18] N. G. McCrum, C. P. Buckley, C. B. Bucknall, *Principles of Polymers Engineering*, New York Oxford Science Publishers, 1997.

